IRAQI JOURNAL OF MATERIALS
Volume (5) Issue (4) October-December 2022, pp. 145-156

Characteristics of Langmuir Probe Diagnostics of Low-Pressure Ar:N_2 Glow Discharge Plasma

Hikmat M. Masroor, Samy A. El-Dardir

Department of Physics, College of Science, University of Sinai, Sinai, EGYPT

Abstract
In this work, experimental results on Langmuir probe diagnostics of low-pressure glow discharge plasma using argon-nitrogen mixtures are presented. The effect of variation in working pressure on the current-voltage characteristics of Langmuir probe diagnostics in unmagnetized glow-discharge plasma was introduced. The current-voltage characteristics of Langmuir probe diagnostics in glow-discharge plasma were studied at working pressure of 0.7mbar and three different cases (no magnetron, using one magnetron at the cathode, and using dual magnetrons). Similarly, the current-voltage characteristics of Langmuir probe in glow-discharge plasma at three different positions of the Langmuir probe inside plasma volume were presented. The variation of electron temperature and density in plasma with working gas pressure at the center point between the electrodes when dual magnetrons were used was determined. As well, the effect of mixing nitrogen with argon on the Langmuir probe characteristics at total working pressure of 0.7mbar and inter-electrode distance of 4cm was studied.

Keywords: Langmuir diagnostics; Plasma parameters; Glow discharge; Sputtering
Received: 15 March 2022; **Revised:** 18 June 2022; **Accepted:** 25 June; **Published:** 1 September 2022

1. Introduction

Probes (initially called “sounding electrodes”) were first used in the late 19th and early 20th centuries in an attempt to measure the voltage distribution in gas discharges and the most important type of probes is Langmuir probe. Langmuir probes are used in low temperature or cold plasmas [1-4] (approximately a few electron volts) to measure some parameters of the plasma, such as plasma density, electron temperature, and plasma potential. Typically, Langmuir probe consists of a bare wire or metal disk, which is inserted into plasma and electrically biased with respect to a reference electrode to collect electron and/or positive ion currents. The use of a cylindrical (wire) probe in a gas discharge tube is shown in figure (1) [5-7]. The case is glow discharge plasma into a glass tube (or other evacuated vessel) with pressures between 10^{-2}−10^{2} mbar. The electric discharge is produced by applying a high DC voltage (300-600V or more) and the corresponding discharge current is in the range of 0.1-100 mA [8].

Langmuir probe is inserted at one or more locations along the length of the tube, with the exposed tip prominent into the plasma column [9]. The early users of Langmuir probe assumed that the potential of the plasma at the probe location (known as the plasma or space potential and designated as V_P) can be determined by measuring the potential on the probe relative to one of the electrodes. However, this procedure determines the floating potential (V_f) of the probe which is in general not the same as the plasma potential. By definition, an electrically floating probe does not collect net current from the plasma, and thus its potential rises and falls to whatever potential is necessary to maintain zero net current [10].

Because of the smaller mass of electrons in typical plasma, they have higher thermal velocities than the positive ions even both are at the same temperature. However, electrons usually have higher temperatures than positive ions [11]. Plasma is electrically neutral by definition and electron and ion densities are nearly equal, however, a floating Langmuir probe will tend to draw higher electron current because they reach the probe faster than ions due to difference in mass [12]. The probe floats to a negative potential relative to the plasma because the net current to the floating probe must be zero, therefore, further collection of electrons is retarded and ion collection is enhanced. This is why the

floating potential is less than that potential of plasma with respect to the walls of the device at a given location in the plasma [13]. Floating potential is generally a few volts positive with respect to the walls because the swifter electrons tend to escape to the walls first, leaving the plasma with a slight excess of positive space charge [14].

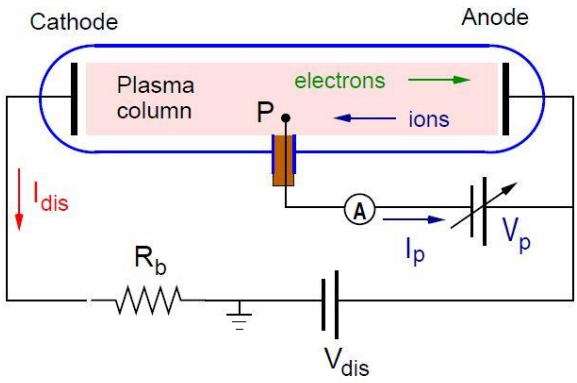

Fig. (1) Schematic diagram of basic gas discharge plasma device at low gas pressure [10]

The bulk of the plasma is "quasineutral" where electron and ion densities are the same, and the potential difference between the bulk of the plasma and the wall is concentrated in a thin layer or sheath near the wall [15]. The gradient of the plasma potential determines the electric field that is responsible for energizing the electrons, which maintain the discharge through ionization [16-18].

Figure (2) shows the typical current-voltage characteristics for Langmuir probe diagnosis of plasma. When the bias voltage (V_B) on the probe is sufficiently negative with respect to the plasma potential (V_P), the probe collects the ion saturation current (I_{is}) and continues to collect positive ions until the bias voltage reaches plasma potential (V_P), at which ions begin to be repelled by the probe. For $V_B >> V_P$, all positive ions are repelled, and the ion current to the probe vanishes (I_i=0).

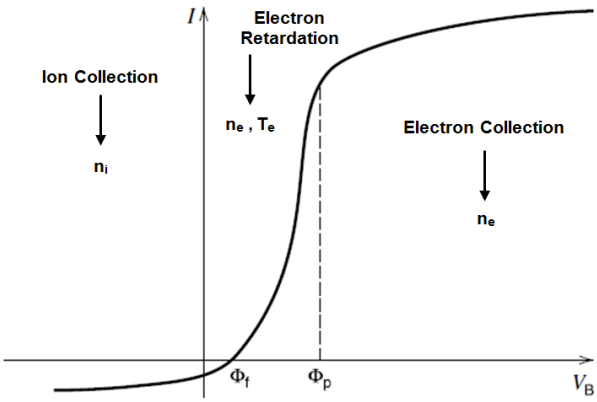

Fig. (2) Typical current-voltage characteristics of Langmuir probe in plasma [16]

For a Maxwellian ion distribution at temperature T_i, the dependence of the ion current $I_i(V_B)$ (usually taken to be the negative current) on V_B is given by [19]

$$I_i(V_B) = \begin{cases} I_{is} exp\left[\frac{e(V_P - V_B)}{k_B T_i}\right] & V_B \geq V_P \\ -I_{is} & V_B < V_P \end{cases} \quad (1)$$

where e is the electron's charge, and k_B is the Boltzmann constant

If ion temperature (T_i) is comparable to electron temperature (T_e), the ion saturation current (I_{is}) is given by [4]

$$I_{is} = \frac{1}{4} e n_i v_{i,th} A_{probe} \quad (2)$$

ISSN (print) 2958-8960 (online) xxxx-xxxx Printed in IRAQ

where n_i is the ion density, $v_{i,th}=(8k_BT_i/\pi m_i)^{1/2}$ is the ion thermal speed, m_i is the ion mass, and A_{probe} is the probe collecting area

If $T_e>>T_i$, the ion saturation current is not determined by the ion thermal speed, but rather is given by the Bohm ion current [20]

$$I_{is} = I_{Bohm} = en_i\sqrt{\frac{k_BT_e}{m_i}}A_{probe}\left[e^{-\frac{1}{2}}\right] = 0.6en_i\sqrt{\frac{k_BT_e}{m_i}}A_{probe} \quad (3)$$

The determination of ion current by the electron temperature when $T_e>>T_i$ is a kind of anticipation and the physical reason for the dependence $I_{is}\sim(k_BT_e/m_i)^{1/2}$ has to do with the formation of a sheath around a negatively biased probe [4]. If an electrode in plasma has a potential different from the local plasma potential, the electrons and ions distribute themselves spatially around the electrode in order to limit, or shield, the effect of this potential on the bulk plasma [21-24]. A positively biased electrode acquires an electron shielding cloud surrounding it, while a negatively biased electrode acquires a positive space charge cloud. For a negatively biased electrode, the characteristic shielding distance of the potential disturbance is the electron Debye length [4,25]

$$\lambda_{De} = \left(\frac{\varepsilon_0 k_BT_e}{e^2n_e}\right)^{1/2} \quad (4)$$

For $V_B>>V_P$ the probe collects electron saturation current (I_{es}). For $V_B<V_P$ the electrons are partially repelled by the probe, and for a Maxwellian electron velocity distribution, the electron current decreases exponentially with decreasing V. For $V_B<<V_P$ all electrons are repelled, so that $I_e=0$. The electron current as a function of V_B can be expressed as

$$I_e(V_B) = \begin{cases} I_{es}exp\left[-\frac{e(V_P-V_B)}{k_BT_e}\right] & V_B \le V_P \\ I_{es} & V_B > V_P \end{cases} \quad (5)$$

The electron saturation current (I_{es}) is given by

$$I_{es} = \frac{1}{4}en_ev_{e,th}A_{probe} \quad (6)$$

where n_e is the electron density, $v_{e,th}\equiv(8k_BT_e/\pi m_e)^{1/2}$ is the electron thermal speed, and m_e is the electron mass

As can be seen from equations (2), (3) and (6), the electron saturation current will be much greater than the ion saturation current because $n_e=n_i$ and $m_e<<m_i$. For example, in an argon plasma where $T_e>>T_i$, according to equations (3) and (6), one can find that

$$\frac{I_{es}}{I_{is}} = \frac{\sqrt{\frac{m_i}{m_e}}}{0.6\sqrt{2\pi}} = \frac{271}{1.5} = 180$$

Table (1) includes parameters of typical laboratory plasma used to construct an ideal Langmuir probe volt-ampere characteristics.

Table (1) Parameters of typical laboratory plasma used to construct an ideal Langmuir probe volt-ampere characteristics [13]

Parameter	Symbol	Value	Units
Ion species	Ar^+		
Ion mass	m_i	6.7×10^{-26}	m^{-3}
Electron density	n_e	1.0×10^{16}	m^{-3}
Ion density	n_i	1.0×10^{16}	m^{-3}
Electron temperature	T_e	2.0	eV
Ion temperature	T_i	0.1	eV
Plasma potential	V_P	1.0	V
Probe diameter	d_{probe}	3.0	mm

2. Experimental Part

The magnetron sputtering system used in this work was designed to include vacuum chamber, discharge electrodes and magnetron assembly, vacuum unit, dc power supplies, gas supply system, cooling system and measuring instruments. The system is schematically shown in figure (3).

The vacuum chamber was constructed from stainless steel. It is a cylinder with internal diameter of 35cm, outer diameter of 45cm, and height of 37.5cm. There were four side holes of 10.8cm in diameter on the circumference of the cylinder; one of them was closed with a quartz window, while the other three were closed with glass windows. These windows were mounted by stainless steel flanges each of 21cm in diameter and four screws. They were used for monitoring the discharge and events

inside the chamber. Each window was far from the discharge region by a neck of 7.5cm diameter to avoid the effects of heat developed by the glow discharge.

The vacuum chamber was sealed from lower end with a stainless steel flange of 40cm in diameter containing a feedthrough for electrical connections required for experiment. The upper end was sealed with a similar flange but containing two feedthroughs; one for gas inlet and Pirani gauge and the other for the Penning gauge. Both flanges include a central hole for the electrode hollow holder. Rubber O-rings and silicon vacuum grease were used in all sealing points.

Both discharge electrodes were constructed from stainless steel (St. St. 304) hollow disks of 80mm in diameter and 8.5mm in thickness. The electrode was joined to holder of 295mm in length and outer and inner diameters of 16.2mm and 11.6mm, respectively, to include a stainless steel channel of 78.5mm in length and 5.6mm in diameter through which the cooling water was flowed to the inside volume of the electrode. The holder tube includes a 1mm-step screw thread of 25.88mm in length to connect the cooling channel tightly.

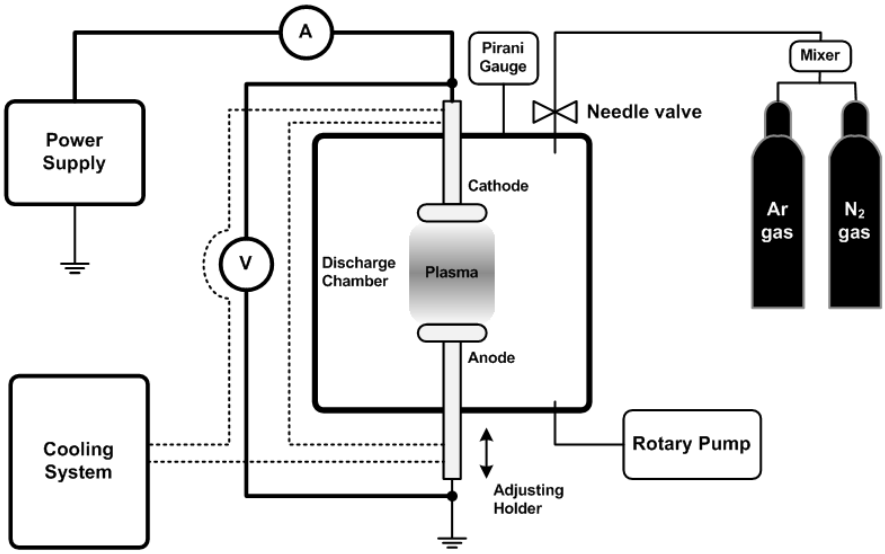

Fig. (3) Schematic diagram of the system used in the present work

Two permanent ring magnets were placed at the back side of each electrode to form the magnetron with a separating distance of 1cm. The inner magnet was 12.5mm in height and 31.5mm in diameter with a central hole of 17.5mm in diameter, while the outer magnet was 15.2mm in height and 80mm in diameter with a central hole of 40mm in diameter. Therefore, the two magnets were separated by a distance of 10mm around their opposing surfaces. A metallic disk of 69.7mm in diameter and 2.5mm in thickness was used to choke the outer magnet to prevent the magnetic field lines from extending to the backside of the electrode.

The design of dual magnetrons proposed in this work provides two concentric regions of high magnetic field intensity on electrode surface. At these regions, the charged particles are totally confined because the particles escaping from the inner region towards the walls of vacuum chamber will lose some energy and then be trapped by the outer region. In conventional configurations, a fraction of charged particles can escape from the confinement region and hence decrease the ionization rate near the cathode.

The advantage of magnetron on the anode is observed in the film deposition of ferromagnetic materials because the magnetic field intensity forces the deposited particles to distribute on the substrate according to its distribution. This makes possible to produce films with selective optical densities to serve multipurpose devices as in the optical data storage applications [26,27].

In order to prevent any variation in the arrangement of internal components, a teflon host of 100mm diameter and 44.5mm height with a central groove of 84.75mm diameter and 26.3mm depth was used to maintain the magnetron from the backside of the electrode. This piece was locked from movement by cylindrical teflon piece of 37.5mm in diameter and 35.25mm in height containing an M5 screw driven towards the holder tube.

A single-stage rotary pump (Leybold-Heraeus) of 9 m^3/hr pumping speed was used to get pressure down to about 10^{-3} mbar inside the vacuum chamber. A water-cooled diffusion pump was available for

use in this work for lower vacuum pressure and connected to the vacuum chamber via a trap. However, all results presented were obtained using the rotary pump only as vacuum pressure of 10^{-2} mbar was easily reached. The minima of Paschen's curves for the inter-electrode distances 2-6 cm were achieved at pressures higher than 10^{-3} mbar. Pirani gauge (down to 10^{-3} mbar) was used.

The electrical power required for generating discharge inside vacuum chamber was provided by a 5 kV dc power supply (Edwards 2A) through high-tension cables. A current-limiting resistance (3.25 k□, 1 kW) was connected between the negative terminal of the dc power supply and the cathode inside the vacuum chamber, while the positive terminal of the dc power supply was connected directly to the anode. The output voltage of the power supply could be varied precisely over 0-5 kV to control the current flowing between discharge electrodes. However, the maximum supply voltage did not exceed 800V. Another dc power supply (0-250 V PHYWE-7532) was used to provide bias potential for Langmuir probe measurements. In addition, a third dc power supply (DHF-1502DD, 1.5-15V, 0.6-2A) was used for electrical measurements performed on the samples prepared as photodetectors.

Gas supply unit consists of argon and nitrogen cylinders, flowmeters, gas flow regulators, needle valves and connections and joints. Argon gas of 96% purity and nitrogen gas of 90% purity were used.

A compact unit was used to cool and circulate the room-temperature water through a channel in discharge electrodes. This unit can cool more than 51 liters of distilled water down to about 4°C and circulate it with maximum flow rate of 30 L/min. The temperature inside the chamber was measured by a thermometer located near the wall of the chamber while the temperatures of both electrodes were measured by thermocouples connected to digital instruments. The maximum surface temperature of the substrate placed on the anode was 40-45°C with uncooled circulating water and reasonably reduced with cooled circulating water.

The operating conditions of the system were classified into two groups; constant and variable. The constant operating conditions include inter-electrode distance, vacuum pressure, current limiting resistance, discharge voltage, discharge current, cooling temperature, cooling water flow rate and deposition time. The variable operating conditions include gas pressure and gas flow rate. Varying discharge voltage was almost possible during the operation. In addition, turning the cooling system off would raise the temperature of either electrode to 40-45°C with circulating water, while stopping the circulation of water would raise electrode temperature more (up to 150°C).

According to the most common assumptions of probe theory, plasma is supposed to be homogenous and its dimensions are large compared to the electron mean free paths, which are inversely proportional to the mean probability of electron collision. In low-pressure plasma (<0.2mbar), the electron mean free paths must be sufficiently long but shorter than the distance between the electrodes.

The plasma parameters are determined from the variation of the probe current (I_p) with the bias voltage ($V-V_p$) as this current is composed of ions, electrons or both. The attracted charges are collected by the probe through the electric field between the bulk plasma and the metallic surface of the probe. This spatial potential profile extends in the plasma along distances in the order of few Debye lengths (λ_D) and is known as "plasma sheath". This local electric field may also be varied according to the magnitude of the probe current (I_p).

Therefore, the charge collection process depends on different characteristic lengths, since the probe size (r_p) and the thickness (or spatial extension) of the plasma sheath is attached to the collecting surface, which relates to λ_D.

In magnetized plasmas, the electron (r_e) and ion (r_i) Larmor radii also introduce additional lengths, as well as the mean free paths (λ) for collisions of electrons and/or ions with neutral atoms in collisional and weakly ionized plasmas.

The idealized situation where the simplified theory strictly applies is seldom found in the experiments of interest. However, even in these situations where different drifting populations of charged particles are present or under intense magnetic fields, the electric probes may provide valuable information [28,29].

As shown before, the probe (P) is immersed at a given point within the plasma biased to the electric potential (V) with respect to a reference electrode. The cathode or the grounded metallic wall of the plasma chamber can also serve for reference electrode in other situations. The current-voltage (I-V) curves are obtained by measuring the drained current (I_p) by the probe for each bias potential (V) and figure (4) represents an idealized current-voltage (I-V) curve.

In order to give a qualitative interpretation, an idealized non-equilibrium collisionless, Maxwellian and unmagnetized plasma will be considered [83]. Thus, the collisional mean free paths of all particles are larger than all characteristic lengths ($\lambda >> r_p, \lambda_D$) and also the electron temperature is higher than those of ions and neutrals ($k_B T_e >> k_B T_i \approx k_B T_a$).

ISSN (print) 2958-8960 (online) xxxx-xxxx Printed in IRAQ

The potential V_p in figure (5) corresponds to the electric potential at the probe insertion point in plasma. The collecting probe does not emit particles, and in accordance to the potential V, the drained current $I_p=I_i+I_e$ from the plasma is composed of ion (I_i) and electron (I_e) currents.

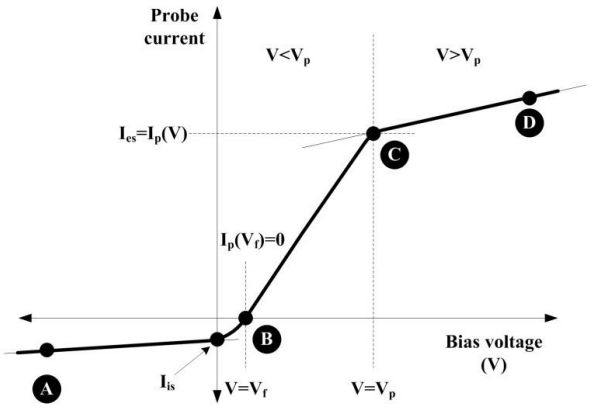

Fig. (4) Idealized I-V characteristics obtained with a collecting Langmuir probe in cold plasma

For very negative bias voltages $V<<V_p$ (at the left of point A in figure (4)) the electrons are repelled and ions are attracted by the probe. The drained ion current from the plasma is limited by the electric shielding of the probe and I_p decreases slowly for very negative $V<<V_p$. The current $I_p \approx I_{is}$ is denominated ion saturation current.

In the opposite limit (voltages at the right of point C in figure (2-7)) where $V>>V_p$, the ions are repelled and the electrons are attracted. In this case, the electrons are responsible for the electric shielding of the probe and $I_p \approx I_{es}$ is called the electron saturation current. The bias potential (V_f) at $I_p=0$ is the floating potential (point B) where the contributions of the ion and electron currents are equal.

The situation of $V<<V_p$ is shown in the scheme of figure (5) where only a small number of electrons have energy enough to jump the potential barrier (V). The ions are attracted to the probe and a layer of negative space charge (negative sheath) develops for $r<r_s$ attached to the metallic surface.

The potential drop from V_p to V and the perturbation caused by the probe electric field is localized within the space charge layer around the probe. It decreases asymptotically in the transition to the unperturbed plasma. In figure (6), the opposite situation with $V>>V_p$ is shown where the electrons are attracted and the negative sheath for $r<r_s$ again connects the space potential of the unperturbed bulk plasma with V.

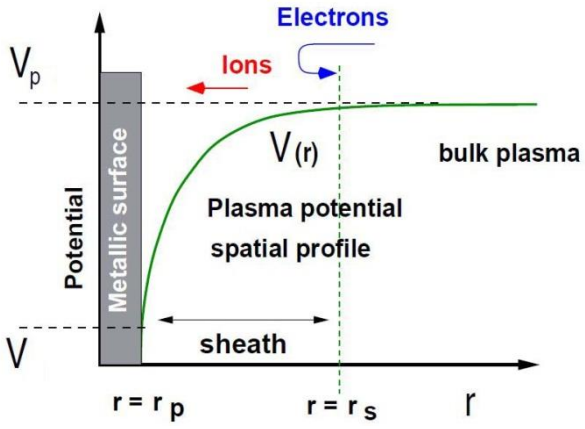

Fig. (5) Radial potential profile attached to an ion collecting metallic surface [14]

The vertical dotted lines in figures (5) and (6) represent external surface of the sheath r_s around the probe. This boundary is not accurately determined and representing the limit beyond which the plasma can be considered quasi-neutral and electric field free. The electrons (or ions) are brought from the

ISSN (print) 2958-8960 (online) xxxx-xxxx Printed in IRAQ

bulk plasma to this boundary mostly by thermal motion. This factor determines the flux of charged particles crossing the radius $r_s > r_p$ towards the probe.

The plasma sheath formed by attracted electrons can be visualized in weakly ionized plasma by bright glow surrounding the cylindrical probe. Because of the large neutral gas atom density, inelastic collisions of neutrals with accelerated electrons in the sheath produce the emission of light. The large electron currents heat the probe and this fact is also used for probe surface cleaning.

On the contrary, the repelled charges with thermal energy sufficient to overcome the potential barrier and reach the probe are collected over its surface. The drained current (I_p) of attracted particles (for either $V >> V_p$ and $V << V_p$) becomes therefore weakly dependent of V as shown in figure (4). This saturation process by attracted particles is in the origin of the currents I_{is} and I_{es} which are the ion and electron saturation currents, respectively.

Finally, when $V = V_p$, no sheath develops around the probe and the charges reach its surface because of their thermal motion. Thus, the probe collects thermal flux of both electrons and ions. In consequence, the probe biased at the space plasma potential drains an electric current from the plasma even in absence of potential difference between the conductor and surrounding plasma.

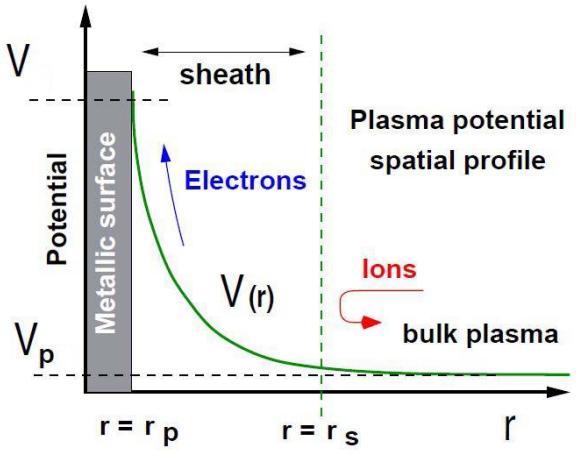

Fig. (6) Radial potential profile attached to electron collecting metallic surface [14]

In order to determine the parameters of the discharge plasma, a homemade Langmuir probe was employed inside the vacuum chamber during the operation of the system, as shown in figure (7). The probe was made from a tungsten wire of 0.4mm in diameter shielded by a glass tube of □-shape and maintained on a stable holder. The tip of the probe was 2mm in length. The position of this tip could be adjusted both vertically and horizontally to probe the plasma at different points.

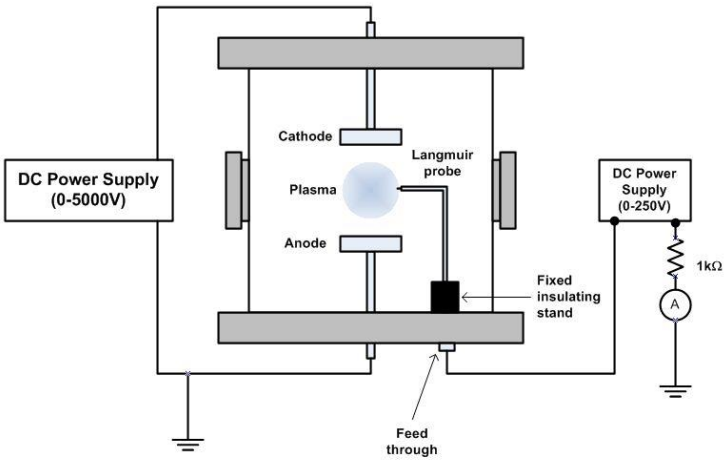

Fig. (7) Schematic diagram of Langmuir probe measurement setup

3. Results and Discussion

The current-voltage characteristics of Langmuir probe diagnostics of unmagnetized glow-discharge plasma at three different working pressures (0.35, 0.7 and 0.9mbar) of argon gas and inter-electrode distance of 4cm are shown in figure (8). In the negative biasing region (ion current region), the current is too small to be noted on the figures at the same scale of electron currents.

At high negative bias voltages, the ion current can be considered equal to saturation ion current (I_{is}). The intersection of this curve with the horizontal axis (bias voltage) gives the value of floating potential ($V_f \approx 5V$), which seems to be stable for this range of working pressures.

Moving to the positive bias voltage region, the electron current is slowly increasing with increasing bias voltage until reaching a point at which, drastic increase in this current is observed. This behavior does not continue as it converts into slow increasing at a certain bias voltage known as “plasma potential” (V_p). At this point, the probe is immersed inside plasma and no sheath develops around the probe and the charges reach its surface because of their thermal motion. Thus, the probe collects the thermal flux of both electrons and ions. In consequence, the probe biased at the space plasma potential drains an electric current from the plasma even in the absence of potential difference between the conductor and the surrounding plasma.

The measured values of floating and plasma potentials for the three working pressures are 5V and 40V, respectively.

All the electrons which acquired energy less than $|eV_b|$ are reflected in the plasma where they can induce new ionizations. Secondary electrons emitted at the substrate electrode are also accelerated towards the plasma and can contribute to ionization enhancement. These secondary electrons are produced mainly by rapid electrons coming from the target.

The increase in the working gas pressure results in measuring higher probe current due to the increasing density of neutral gas atoms those subjected to collisions with the available charged particles and hence producing much more charged particles to compose the drained current (I_p). However, the behaviors of these characteristics are identical with upward shift at higher pressures.

In order to clarify the effects of using magnetrons on the parameters of plasma, the Langmuir probe measurements were performed at working pressure of 0.7mbar when only one magnetron was used at the cathode and when dual magnetrons used and then compared to those obtained when no magnetron used, as shown in figure (9).

It is clear that using only one magnetron at the cathode caused to decrease the drained current by the probe by about 12%. This decrease may be attributed to the role of this magnetron in trapping a fraction of the electrons in the discharge volume near the cathode to increase the ionization rate of the neutral gas atoms, and hence preventing the probe from collecting more electrons.

In case of using dual magnetrons, the drained current by the probe was decreased by about 16% due to the roles of both magnetrons in trapping much more charged particles near the cathode and anode and hence reducing the number of particles passing the distance between the electrodes where the probe is placed. However, these roles could not prevent the discharge current from flowing between the electrodes but even these particles sustaining the discharge are accelerated by the both electric and magnetic fields to higher drift velocities that the probe could not attract them from their paths across the inter-electrode distance.

Accordingly, the magnetrons changed the values of plasma parameters, such as electron and ion temperatures and densities, as these parameters are deduced from the current-voltage characteristics of the probe immersed in plasma. These variations are observed in Table (2).

ISSN (print) 2958-8960 (online) xxxx-xxxx Printed in IRAQ

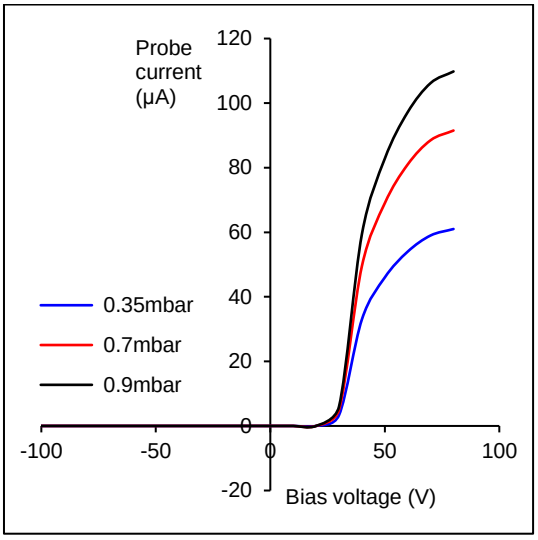

Fig. (8) Effect of variation in working pressure on the current-voltage characteristics of Langmuir probe diagnostics in unmagnetized glow-discharge plasma

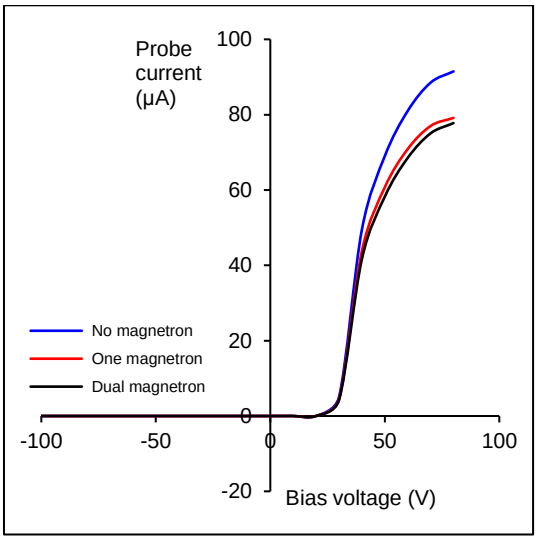

Fig. (9) Current-voltage characteristics of Langmuir probe diagnostics in glow-discharge plasma at working pressure of 0.7mbar and three different cases (no magnetron, using one magnetron at the cathode, and using dual magnetrons)

Table (2) Effect of using magnetrons on the plasma parameters at working pressure of 0.7mbar and the probe placed at the center point between the electrodes

	Without magnetron	One magnetron	Dual magnetrons
Electron temperature (eV)	4.8566	4.871	4.850
Electron density ($x10^{21}m^{-3}$)	1.329	1.148	1.130
Ion temperature (eV)	0.889-1.192	0.888-1.189	0.864-1.159
Ion density ($x10^{21}m^{-3}$)	1.329	1.148	1.130

The measurements described in Section 3.5.2 were repeated when the probe placed near each of the electrodes (cathode and anode) and at the center point in case of dual magnetrons in order to determine the plasma parameters at this position, as shown in figure (10).

The probe current near the cathode was higher than other positions because the densities of electrons are higher than any other regions inside plasma, since the cathode is the source of discharge electrons in addition to the trapping effect of the magnetron placed at the cathode.

Therefore, the probe would collect much more electrons in this region. The increase in probe current near the cathode was about 46% than its value at the center point between the electrodes. The probe current near the anode was higher by about 6% than its value at the center point because the density of electrons near the anode is already low and the magnetron at the anode also plays a role in trapping a fraction of these electrons near the anode. Therefore, the number of electrons detected by the probe near the anode is reasonably lower than that near the cathode.

For comparison, the electron temperatures and densities were determined from the current-voltage characteristics of Langmuir probe studied with different working gas pressures at the center point between the electrodes. As shown in figures (11), the electron temperature was reduced as the working pressure increased from 0.35 to 0.7mbar and then raised as the pressure increased from 0.7 to 0.9 mbar.

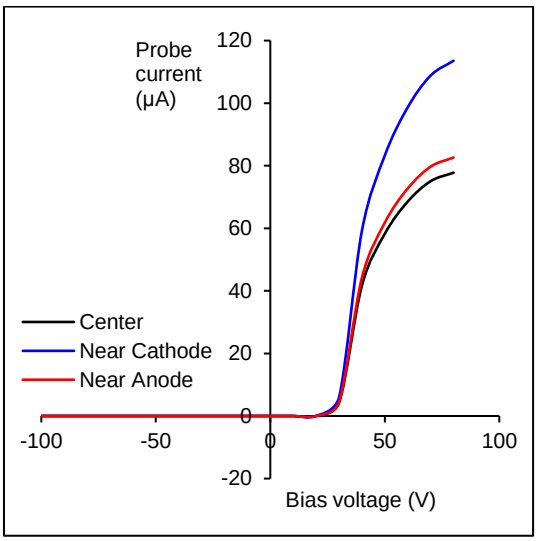

Fig. (10) Current-voltage characteristics of Langmuir probe in glow-discharge plasma at three different positions of the Langmuir probe inside plasma volume

The further increase of working pressure (to 0.9 mbar) provided the discharge volume with more neutral gas atoms, therefore, the number of collisions among electrons and neutral atoms is increased and hence the production of charged particles is increased too. Accordingly, the electron density is increased and more electrons are trapped by $\vec{E} \times \vec{B}$ effect before escaping to pass the inter-electrode distance as well as the center point where the probe is placed. These electrons are relatively higher in energy than those escaping at lower pressures (0.7mbar) because they were initially trapped before the electron density being higher than the capability of trapping region. Therefore, the probe would detect more electrons with higher energies (temperatures).

Despite that ion temperatures are much lower than electron temperatures; similar behavior was observed when measured at different points between the electrodes. On the other hand, the electron density as well as ion density was continuously increased with increasing working pressure due to the corresponding increase in discharge current, as shown earlier. Table (3) includes the plasma parameters deduced at three different positions between the discharge electrodes. Each value is an average of several values obtained from different experiments.

Increasing the working pressure means providing the discharge volume with more neutral atoms of argon and hence the mean free path of electrons as well as their gained energy is reduced as the number of their collisions with neutral atoms is decreased. Accordingly, the number of electrons produced by collisional ionization processes is decreased. The majority of these electrons are trapped by the magnetrons at both electrodes while the minority of electrons may escape from the trapping region towards the anode to sustain the glow discharge with lower energies (lower temperatures) than those trapped because they will be subject only to the electric field between the electrodes (*V/d*) while those trapped near the electrodes are subject to $\vec{E} \times \vec{B}$ drift.

ISSN (print) 2958-8960 (online) xxxx-xxxx Printed in IRAQ

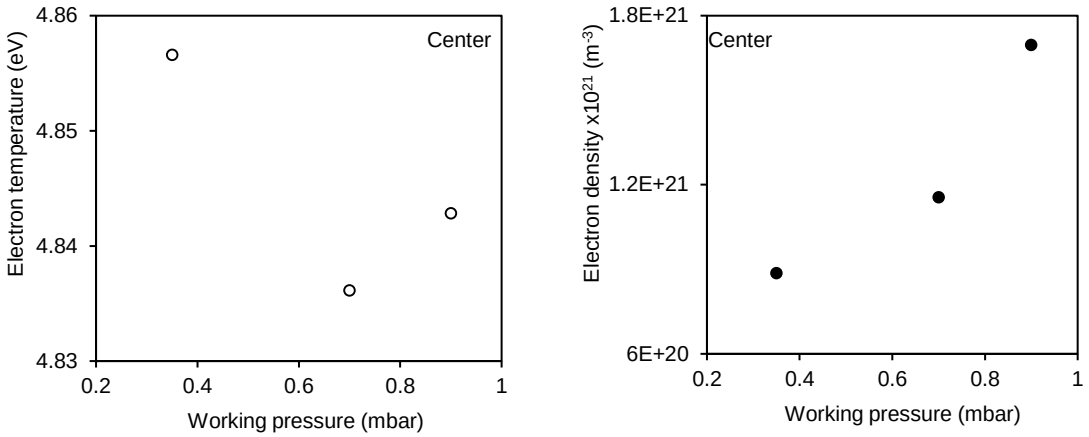

(a) **(b)**

Fig. (11) Variation of electron temperature and density in plasma with working gas pressure at the center point between the electrodes when dual magnetrons were used

Table (3) Plasma parameters measured at working gas pressure of 0.7mbar and three different positions between the discharge electrodes

	Center point	Near cathode	Near anode
Electron temperature (eV)	4.856	4.838	4.855
Electron density (x10^{21}m^{-3})	1.130	1.654	1.201
Ion temperature (eV)	0.864-1.159	0.885-1.188	0.869-1.166
Ion density (x10^{21}m^{-3})	1.130	1.654	1.201

A fraction of the electrons escaping from $\vec{E} \times \vec{B}$ trapping region may be collected by the probe at the center point between the electrodes to form the probe current, which was lower than that near the electrodes.

The current-voltage characteristics of Langmuir probe diagnostics of unmagnetized glow-discharge plasma for two different cases (Ar gas and Ar:N_2 mixture) at working pressure of 0.7 mbar are shown in figure (12). An increase in the probe current can be observed for the Ar:N_2 mixture due to the increase in collisional ionization coefficients in the presence of the nitrogen molecules added to argon.

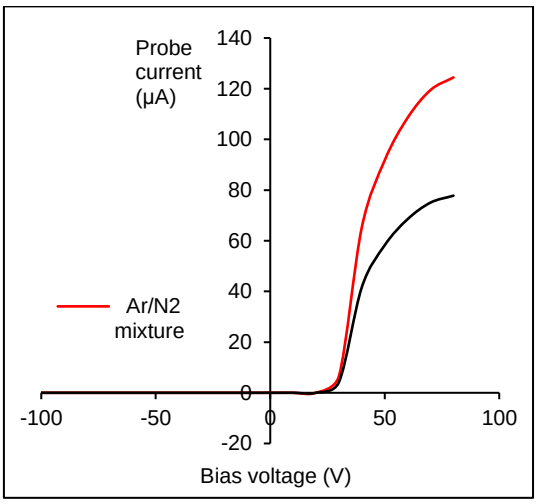

Fig. (12) Effect of mixing nitrogen with argon on the Langmuir probe characteristics at total working pressure of 0.7mbar and inter-electrode distance of 4cm

In the negative biasing region (ion current region), the current is too small to be noted on the figures at the same scale of electron currents. At high negative bias voltages, the ion current is about the same as that of the saturation ion current (I_{is}). The intersection of this curve with the horizontal axis

(bias voltage) gives the value of floating potential (V_f ≈5V), which seems to be stable for this range of working pressures. Table (4) explains the effect of using N_2:Ar mixture on the plasma parameters.

Table (4) Effect of using nitrogen:argon mixture on the plasma parameters

Dual magnetrons	Ar gas only	Ar:N_2 mixture
Electron temperature (eV)	4.8504821	4.837
Electron density (x$10^{21}m^{-3}$)	1.130	1.811
Ion temperature (eV)	0.864-1.159	0.865-1.164
Ion density (x$10^{21}m^{-3}$)	1.130	1.329

References

[1] F. Ghaleb and A. Belasri, Radiation Effects and Defects in Solids, 1, 1-7 (2012).
[2] M.A. Lieberman and A.J. Lichtenberg, Principles of Plasma Physics and Materials Processing, Second edition, Wiley, p. 547 (2005).
[3] R.L. Merlino, Am. J. Phys., 75(12), 1078-1085 (2007).
[4] L. Conde, An introduction to Langmuir probe diagnostics of plasmas, Departamento de Física Aplicada, Universidad Politécnica de Madrid, Spain (2011), online article.
[5] E.V. Shun'ko, Langmuir Probe in Theory and Practice (contents and introduction only), Universal Publishers, Boca Raton, Florida, USA (2008).
[6] P. Vǎsina, Plasma diagnostics focused on new magnetron sputtering devices for thin film deposition, PhD thesis, Universit´e Paris-Sud XI, France & Masaryk University in Brno, Czech Republic, pp. 12-19 (2005).
[7] M.M. Mansour, N.M. El-Sayed, O.F. Farag and M.H. Elghazaly, Arab J. of Nuclear Sci. and Applications, 46(1), 116-125 (2013).
[8] I. Svadkovski, D. Golosov and S. Zavatskiy, Vacuum, 68, 283–290 (2003).
[9] A.A. Solov'ev, Plasma Phys. Rep., 35(5), 399–408 (2009).
[10] A. Bojarov, M. Radmilovic-Radjenovic and Z. Petrovic, Effect of the ion induced secondary electron emission on the characteristics of RF plasmas, Publ. Astron. Obs. Belgrade, 89, 131-134 (2010).
[11] A.R. Gonzalez-Elipe, F. Yubero and J.M. Sanz, Low Energy Ion Assisted Film Growth, Imperial College Press, p. 110 (2003).
[12] T.E. Sheridan, M.J. Goeckner and J. Goree, J. Vac. Sci. Technol. A, 8(1), 30-37 (1990).
[13] J.W. Bradley, J. Phys. D: Appl. Phys., 25, 1443-1453 (1992).
[14] M.B. Hendricks, J. Vac. Sci. Technol. A 12, 1408 (1994)
[15] M. Tichý, J. Phys. IV France, 7, C4-397-411 (1997).
[16] T.E. Sheridan, M.J. Goeckner and J. Goree, J. Vac. Sci. Technol. A 16(4), 2173-2176 (1998).
[17] C. Engström, Vacuum, 56, 107-113 (2000).
[18] E. Martines, Phys. of Plasmas, 8(6), 3042-3050 (2001).
[19] C.H. Shon and J.K. Lee, Appl. Surf. Sci., 192, 258-269 (2002).
[20] I. Levchenko, Appl. Phys. Lett., 85(12), 2202-2204 (2004).
[21] G. Petraconi, Brazilian J. of Physics, 34(4B), 1662-1666 (2004).
[22] H. Yasuda, L. Ledernez, F. Olcaytug and G. Urban, Pure Appl. Chem, 80(9), 1883-1892 (2008).
[23] Milan Tichý, J. Plasma Fusion Res. SERIES, 8, 1277-1282 (2009).
[24] M. Yusupov, New J. of Physics, 13, 033018 (2011).
[25] M. Yusupov, Appl. Phys. Lett., 98, 131502 (2011).
[26] M.A. Hassouba and N. Dawood, Adv. in Appl. Sci. Res., 2(4), 123-131 (2011).
[27] E.F. Kotp and A.A. Al-Ojeery, Australian J. of Basic and Appl. Sci., 6(3), 817-825 (2012).
[28] Karol Macak, J. Vac. Sci. Technol. A 18(4), 1533-1537 (2000).
[29] D.M. Goebel and I. Katz, Basic Plasma Physics (Chapter 3), Fundamentals of Electric Propulsion: Ion and Hall Thrusters, John Wiley & Sons, p. 80 (2008).

 ISSN (print) 2958-8960 (online) xxxx-xxxx Printed in IRAQ